

# Nanographite Impurities Dominate Electrochemistry of Carbon Nanotubes

Adriano Ambrosi<sup>[b]</sup> and Martin Pumera<sup>\*[a]</sup>

*Dedicated to Professors Miroslava Harnová, Jana Becková and Alena Ledinská*

Carbon nanotubes (CNTs) and related materials are in the forefront of research in a wide variety of fields. CNTs have been employed in biosensors, fuel cells, and energy storage devices, typically utilizing their electrochemical properties.<sup>[1,2]</sup> The application of the electrochemistry of CNTs has been studied in detail and it has been demonstrated that CNT-based materials decrease overpotential for the oxidation/reduction of many important compounds, increase voltammetric current, exhibit an “electrocatalytic effect”, and show negligible electrode surface fouling.<sup>[1,2]</sup>

It is well known that CNTs are highly heterogeneous materials, containing significant amounts of amorphous carbon, crystalline nanographite particles,<sup>[3]</sup> and residual metallic catalyst impurities.<sup>[4]</sup> Compton et al. first demonstrated that residual metallic impurities within CNTs are responsible for the reported electrocatalytic effect on the oxidation of hydrazine<sup>[5]</sup> and glucose<sup>[6]</sup> and on the reduction of hydrogen peroxide.<sup>[7]</sup> We have shown that metallic impurities within CNTs participate in the redox behavior of amino acids<sup>[8]</sup> and regulatory proteins,<sup>[9]</sup> even at concentrations in the order of hundreds of ppm ( $\approx 0.01$  wt %)<sup>[10]</sup> and we elucidated the role of multicomponent metallic impurities.<sup>[10,11]</sup> However, the influence of carbon-based impurities upon the electrochemical behavior of CNTs has not received similar attention.

It is generally perceived that the electrochemistry of CNTs is comparable to that of graphite, with an analogous voltammetric response.<sup>[12]</sup> Herein, we wish to challenge this

view and prove that the observed heterogeneous electron-transfer (HET) rate of CNT materials is comparable to that of graphite only because CNT materials contain large quantities of nanographite impurities. When pure CNTs are used, the observed HET rate is actually significantly lower than that of graphitic materials. In other words, most of the electrochemical activity of CNTs is due to the presence of the nanographite impurities contained within them.

It has been proven for  $sp^2$ -hybridized carbon materials (such as graphite) that HET is fastest at the edges of a graphene sheet (observed HET rate constant,  $k_{\text{obs}}^0$ , is in the range of  $0.01 \text{ cm}^2 \text{ s}^{-1}$ ), whereas it is very slow ( $k_{\text{obs}}^0$  is less than  $10^{-7}$  and likely approaching zero, although the exact value is still discussed in the literature) at the basal plane.<sup>[13–17]</sup> When HET occurs at the basal plane, it is only because of defects present at such planes.<sup>[13–16]</sup> It has been found that this is also true for CNTs, in which the open ends provide fast HET, whereas HET at the CNT walls is negligible, even for small-diameter single-walled CNTs (SWCNTs), in which the curvature effect could possibly have played a role.<sup>[18,19]</sup>

When considering the structure of CNTs (Figure 1) and comparing it with graphite/nanographite, one might wonder why were CNTs deemed to exhibit fast HET at all, since the ideal defect-free CNTs have electrochemically active sites only at the ends of the nanotube, contrary to nanographite, where the concentration of edge-plane sites (per gram of material) in (nano)graphite is much higher.

Indirect evidence has been mounting that carbon-impurity-free CNTs actually do not exhibit fast HET rates at all. Li's group compared the electrochemical performance of CNTs with that of graphene nanomaterials (note that such graphene nanomaterials were prepared by techniques that lead to multilayer graphene structures similar to nanographite) and found that the HET rate on such multilayer graphene is faster than that of SWCNTs.<sup>[20]</sup> Similarly, we found that stacked graphene platelet nanofibers exhibit faster HET than MWCNTs.<sup>[21]</sup>

Herein, we demonstrate by means of the controlled introduction of nanographite impurities into carbon-impurity-free CNTs that the HET rate of such CNT samples is gov-

[a] Prof. M. Pumera  
School of Physical and Mathematical Sciences  
Division of Chemistry and Chemical Biology  
Nanyang Technological University  
21 Nanyang Link (Singapore)  
Fax: (+65) 6791-1961  
E-mail: martin.pumera@gmail.com  
pumera@ntu.edu.sg

[b] Dr. A. Ambrosi  
Biomaterials Center, National Institute for Materials Science  
1-1 Namiki, Tsukuba, Ibaraki (Japan)

Supporting information for this article is available on the WWW under <http://dx.doi.org/10.1002/chem.201001584>.

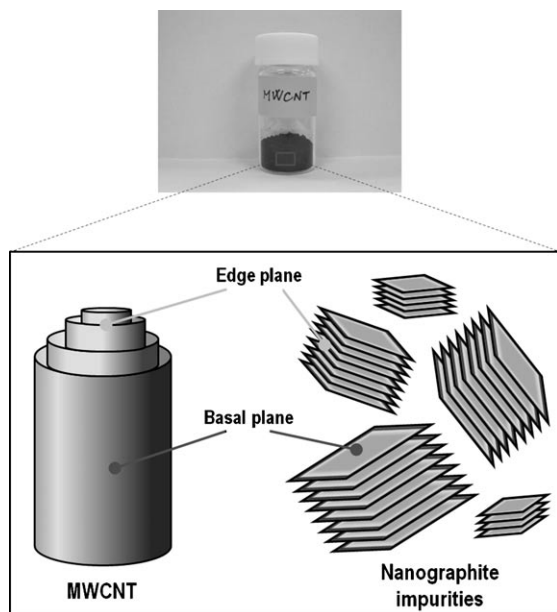


Figure 1. Schematic drawing of multiwalled CNT (MWCNT; left) and nanographite impurities (right). Note that the fast HET occurs on the nanographite edges and CNT ends, whereas the nanographite basal planes and the CNT sides exhibit a significantly lower rate of heterogeneous electron transfer.

erned by the amount of nanographite impurities. We used two types of carbon-impurity-free CNTs (based on provider information and our TEM characterization), referred to as MWCNT-A and MWCNT-B (for detailed characterization of these CNTs, please see the Experimental Section), to prove that our conclusions are not specific to one particular type of CNT. In addition, we controllably introduced nanographite (NG) and graphite microparticles (GMP) into them and recorded cyclic voltammograms of a ferricyanide probe to establish the observed HET rate constant ( $k_{\text{obs}}^0$ ). Both MWCNT-A and MWCNT-B were open-ended CNTs.<sup>[4,16]</sup>

Figure 2 shows selected cyclic voltammograms of MWCNT-A containing 0 to 30 wt % of NG impurities and of 100 % NG. The decrease in peak-to-peak separation signifies an increase in the HET rate. It is clearly evident that with an increasing amount of NG “impurities” introduced into pure MWCNT-A  $k_{\text{obs}}^0$  increases from  $1.7 \times 10^{-5} \text{ cm s}^{-1}$  for pure MWCNT-A to  $6.0 \times 10^{-4} \text{ cm s}^{-1}$  for 10 wt % of NG impurities in MWCNT-A and further to  $1.7 \times 10^{-3} \text{ cm s}^{-1}$  for 30 wt % of NG impurities in the MWCNT-A sample. Figure 3 graphically illustrates the influence of the amount of NG and GMP impurities in MWCNT-A on the peak-to-peak separation of the oxidation/reduction peaks of  $[\text{Fe}(\text{CN})_6]^{3-/4-}$  and calculated  $k_{\text{obs}}^0$  based on Nicholson's method.<sup>[22]</sup> It is interesting to note that the value of  $k_{\text{obs}}^0$  for 25 wt % NG impurities in the MWCNT-A sample is actually very close to the value found for 100 wt % of NG impurities. This shows that at concentrations around 25 wt %, the NG impurities actually dominate the electrochemistry of CNT materials. Note that typical commercial MWCNT samples

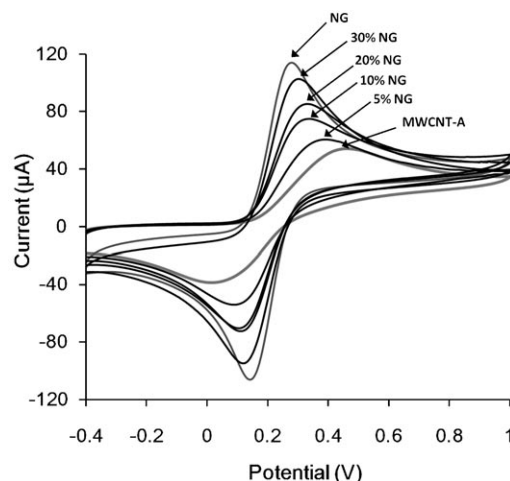


Figure 2. Cyclic voltammograms of CNTs (MWCNT-A) with different ratios of NG impurities. Note that peak-to-peak separation of oxidation and reduction of  $[\text{Fe}(\text{CN})_6]^{3-/4-}$  decreases significantly even at 5 wt % of impurities present in the sample, signifying that NG impurities have a profound influence upon the electrochemistry of CNTs even at low concentrations.

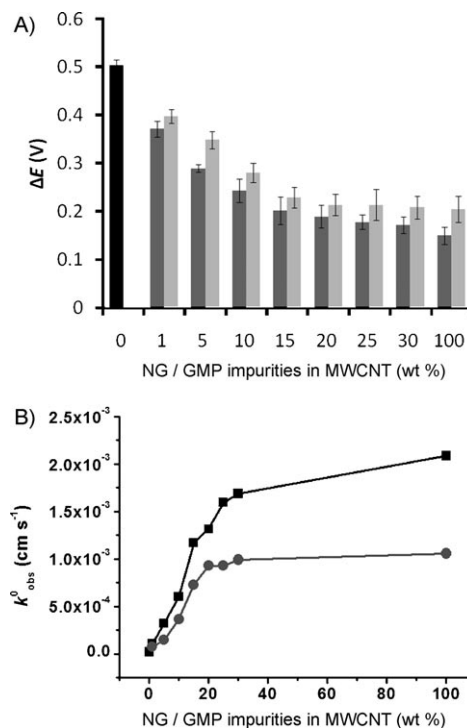


Figure 3. Effect of the presence of NG and GMP impurities in the CNT sample upon the electrochemical behavior towards oxidation/reduction of 10 mM  $[\text{Fe}(\text{CN})_6]^{3-/4-}$  in 0.05 M PBS buffer (pH 7.2). A) peak-to-peak separation (black: pure MWCNT-A; dark gray: MWCNT-A with NG, and light gray: MWCNT-A with GMP). Decreasing peak-to-peak separation indicate faster HET. B) Resulting  $k_{\text{obs}}^0$  for MWCNT-A containing different amounts of NG (■) and GMP (●) impurities.

contain about 10–20 wt % of NG impurities, while typical SWCNT samples contain 30–40 % of NG impurities.<sup>[23]</sup> Therefore, it is clear that in typical commercial samples of CNTs, the electrochemistry of CNTs is likely to be governed

by NG impurities, not by the CNTs themselves. To verify this by using different “impurities”, we repeated the same experiments with GMP-simulating impurities. We observed behavior analogous to that of NG impurities. The  $k_{\text{obs}}^0$  value increases from  $1.7 \times 10^{-5} \text{ cm s}^{-1}$  for pure MWCNT-A to  $3.6 \times 10^{-4} \text{ cm s}^{-1}$  for 10% of GMP impurities in MWCNT-A, continuing to increase to  $9.3 \times 10^{-4} \text{ cm s}^{-1}$  for 20 wt% of GMP impurities, and then levels off, exhibiting  $k_{\text{obs}}^0$  of  $9.9 \times 10^{-4} \text{ cm s}^{-1}$  for 30 wt% of GMP impurities. The  $k_{\text{obs}}^0$  value for a 100% GMP-modified electrode resulted in only a slightly higher value of  $1.1 \times 10^{-3} \text{ cm s}^{-1}$ . Again, GMP completely dominates the electrochemistry of MWCNT-A at a concentration of 20 wt%. To prove that this is a general case, not just related to the specific MWCNT sample under investigation, we employed another carbon-impurity-free MWCNT (MWCNT-B), which was obtained from a different supplier. We observed very similar trends upon introduction of the NG and GMP impurities, as shown in Figure SI-1 (see the Supporting Information). Note that all presented  $k_{\text{obs}}^0$  values are averages of six measurements recorded using different electrodes.

In conclusion, we demonstrated that the electrochemistry of MWCNTs could be dominated by the presence of NG/GMP impurities, which have a much higher edge-plane/weight ratio than CNTs. We also demonstrated that before attributing the observed fast HET kinetics to the CNTs, the CNT samples should be purified not only with regard to the presence of metallic impurities, but equally importantly with regard to the presence of NG/GMP impurities. The most important implication of our research is that since pure CNTs do not provide fast HET kinetics, but instead such properties originate in the NG and GMP impurities within the CNTs, it might be more beneficial in some cases to employ NG materials, such as graphite nanofibers or nanoplatelets for the construction of high-performance electrochemical sensing and energy-storage devices, instead of CNTs. Indeed, MWCNTs still have important properties as conductors or support materials, that is, they may serve as conductive nanowire scaffolds to provide heterogeneous supports to catalysts (controlling the morphology and increasing the surface area of the resulting nanostructured hybrid material) and to funnel the sequential electron transfer to the electrode, favoring energy dispersion and relieving catalytic fatigue and thus they will still find areas of application in electrochemistry.

## Experimental Section

**Apparatus:** All voltammetric experiments were performed by using an electrochemical analyzer Autolab 302 (Ecochemie, Utrecht, The Netherlands) connected to a PC and controlled by General Purpose Electrochemical Systems v. 4.9 software (Ecochemie). The electrochemical experiments were carried out in a 5 mL voltammetric cell at room temperature (25 °C) using a three-electrode configuration. A platinum electrode served as an auxiliary electrode and a Ag/AgCl electrode as a reference electrode.

**Materials:** Potassium chloride, potassium phosphate, disodium salt, potassium ferrocyanide, potassium ferricyanide, and phosphoric acid were purchased from Sigma-Aldrich (Japan). MWCNTs were purchased from Sigma Aldrich (MWCNT-A) and Bucky, TX, USA (MWCNT-B). Both MWCNT-A and -B were open-ended (representative TEM images can be found in our previous publications, see references [24] and [16], respectively). MWCNT-A had a diameter of 90–110 nm, a length of 5–9  $\mu\text{m}$ , and contained <3 ppm Fe-based impurities; MWCNT-B had a diameter of 8–15 nm and a length of 5–10  $\mu\text{m}$ . Both MWCNT samples were characterized extensively by using TEM and thermogravimetric analysis (TGA; see Figure SI-2 in the Supporting Information).<sup>[3]</sup> Both methods proved that there are no carbonaceous impurities within the samples MWCNT-A and B. GMP (particle size  $\approx 20 \mu\text{m}$ ) and NG nanofibers (fiber diameter  $\approx 80 \text{ nm}$ ) were obtained from Sigma-Aldrich.

**Procedures:** Carbon materials were used as received without further purification and nitric acid treatment. For the electrochemistry measurements, the CNTs and graphite impurity solutions were prepared at the required ratios by dispersion in DMF at a total concentration of  $1 \text{ mg mL}^{-1}$ . After sonication for 5 min, 5  $\mu\text{L}$  of the suspension was pipetted on the glassy carbon (GC) electrode surface (3 mm in diameter, surface area of  $0.071 \text{ cm}^2$ , received from Autolab), which was previously polished with  $0.05 \mu\text{m}$  alumina on a polishing cloth. The carbon material suspension deposited on the GC electrode was allowed to evaporate at room temperature, creating a MWCNT film over the whole GC electrode surface. The NG and GMP impurities were physically introduced in the CNT samples and such samples were consequently treated in the same way as pure CNTs. Cyclic voltammetric experiments were performed at a scan rate of  $100 \text{ mV s}^{-1}$  over a relevant potential range using  $0.05 \text{ M}$  phosphate buffer solution (pH 7.2).  $[\text{Fe}(\text{CN})_6]^{3-/4-}$  was used as an electrochemical probe at a concentration of  $10 \text{ mM}$  unless stated otherwise.

The  $k_{\text{obs}}^0$  values were determined by using the method developed by Nicholson<sup>[22]</sup> that relates  $\Delta E_p$  to dimensionless parameter  $\psi$  and consequently to  $k_{\text{obs}}^0$  through Equation (1):

$$k_{\text{obs}}^0 = \psi \sqrt{\pi D_A \nu \frac{nF}{RT}} \quad (1)$$

in which  $k_{\text{obs}}^0$  is the observed heterogeneous rate constant,  $D_A$  is the diffusion coefficient,  $\nu$  is the scan rate,  $F$  is the Faraday constant,  $R$  is the gas constant, and  $T$  is the absolute temperature. The value of  $\psi$  and a detailed discussion on the use of this equation can be obtained from the literature.<sup>[22]</sup> The roughness factor was not taken into account. Since all  $k_{\text{obs}}^0$  data are obtained by either interpolation (for  $\Delta E_p$  between 60 and 242 mV) or extrapolation (for  $\Delta E_p > 242 \text{ mV}$ ) of Nicholson's working curve,<sup>[22]</sup> an additional interpolation/extrapolation error of approximately 0–2% was introduced in addition to the experimental error of  $\Delta E_p$ . It should be noted that there could be many redox systems that do not follow the reactivity pattern of ferrocyanide.

## Acknowledgements

This work was partially supported by NAP start-up fund (grant no. M58110066) provided by NTU.

**Keywords:** carbon nanotubes • electrochemistry • electron transfer • nanostructures

- [1] a) I. Dumitrescu, P. R. Unwin, J. V. Macpherson, *Chem. Commun.* **2009**, 6886; b) L. Kavan, L. Dunsch, *ChemPhysChem* **2007**, *8*, 974; c) J. J. Gooding, *Electrochim. Acta* **2005**, *50*, 3049.
- [2] M. Pumera, *Chem. Eur. J.* **2009**, *15*, 4970.
- [3] M. E. Itkis, D. E. Perea, R. Jung, S. Niyogi, R. C. Haddon, *J. Am. Chem. Soc.* **2005**, *127*, 3439.

- [4] a) T. Kolodiazny, M. Pumera, *Small* **2008**, *4*, 1476; b) M. Pumera, *Langmuir* **2007**, *23*, 6453.
- [5] C. E. Banks, A. Crossley, C. Salter, S. J. Wilkins, R. G. Compton, *Angew. Chem.* **2006**, *118*, 2595; *Angew. Chem. Int. Ed.* **2006**, *45*, 2533.
- [6] C. Batchelor-McAuley, G. G. Wildgoose, R. G. Compton, L. Shao, M. L. H. Green, *Sens. Actuators B* **2008**, *132*, 356.
- [7] B. Šljukić, C. E. Banks, R. G. Compton, *Nano Lett.* **2006**, *6*, 1556.
- [8] M. Pumera, H. Iwai, Y. Miyahara, *ChemPhysChem* **2009**, *10*, 1770.
- [9] A. Ambrosi, M. Pumera, *Chem. Eur. J.* **2010**, *16*, 1786.
- [10] a) M. Pumera, H. Iwai, *Chem. Asian J.* **2009**, *4*, 554; b) M. Pumera, Y. Miyahara, *Nanoscale* **2009**, *1*, 260.
- [11] M. Pumera, H. Iwai, *J. Phys. Chem. C* **2009**, *113*, 4401.
- [12] R. R. Moore, C. E. Banks, R. G. Compton, *Anal. Chem.* **2004**, *76*, 2677.
- [13] T. J. Davies, M. E. Hyde, R. G. Compton, *Angew. Chem.* **2005**, *117*, 5251; *Angew. Chem. Int. Ed.* **2005**, *44*, 5121.
- [14] R. J. Bowling, R. T. Packard, R. L. McCreery, *J. Am. Chem. Soc.* **1989**, *111*, 1217.
- [15] R. J. Rice, R. L. McCreery, *Anal. Chem.* **1989**, *61*, 1637.
- [16] M. Pumera, T. Sasaki, H. Iwai, *Chem. Asian J.* **2008**, *3*, 2046.
- [17] I. Dumitrescu, P. V. Dudin, J. P. Edgeworth, J. V. Macpherson, P. R. Unwin, *J. Phys. Chem. C* **2010**, *114*, 2633.
- [18] A. F. Holloway, G. G. Wildgoose, R. G. Compton, L. Shao, M. L. H. Green, *J. Solid State Electrochem.* **2008**, *12*, 1337.
- [19] A. F. Holloway, K. Toghill, G. G. Wildgoose, R. G. Compton, M. A. H. Ward, G. Tobias, S. A. Llewellyn, B. Ballesteros, M. L. H. Green, A. Crossley, *J. Phys. Chem. C* **2008**, *112*, 10389.
- [20] S. Alwarappan, A. Erdem, C. Liu, C.-Z. Li, *J. Phys. Chem. C* **2009**, *113*, 8853.
- [21] A. Ambrosi, T. Sasaki, M. Pumera, *Chem. Asian J.* **2010**, *5*, 266.
- [22] R. S. Nicholson, *Anal. Chem.* **1965**, *37*, 1351.
- [23] P.-X. Hou, C. Liu, H.-M. Cheng, *Carbon* **2008**, *46*, 2003.
- [24] M. Pumera, B. Šmíd, X. Peng, D. Golberg, J. Tang, I. Ichinose, *Chem. Eur. J.* **2007**, *13*, 7644.

Received: June 7, 2010  
Published online: August 16, 2010